Fourier and Real Time Diffractometry at the IBR-2 and Science

Sergey Sumnikov

Correlation Fourier diffractometry at the IBR-2 reactor

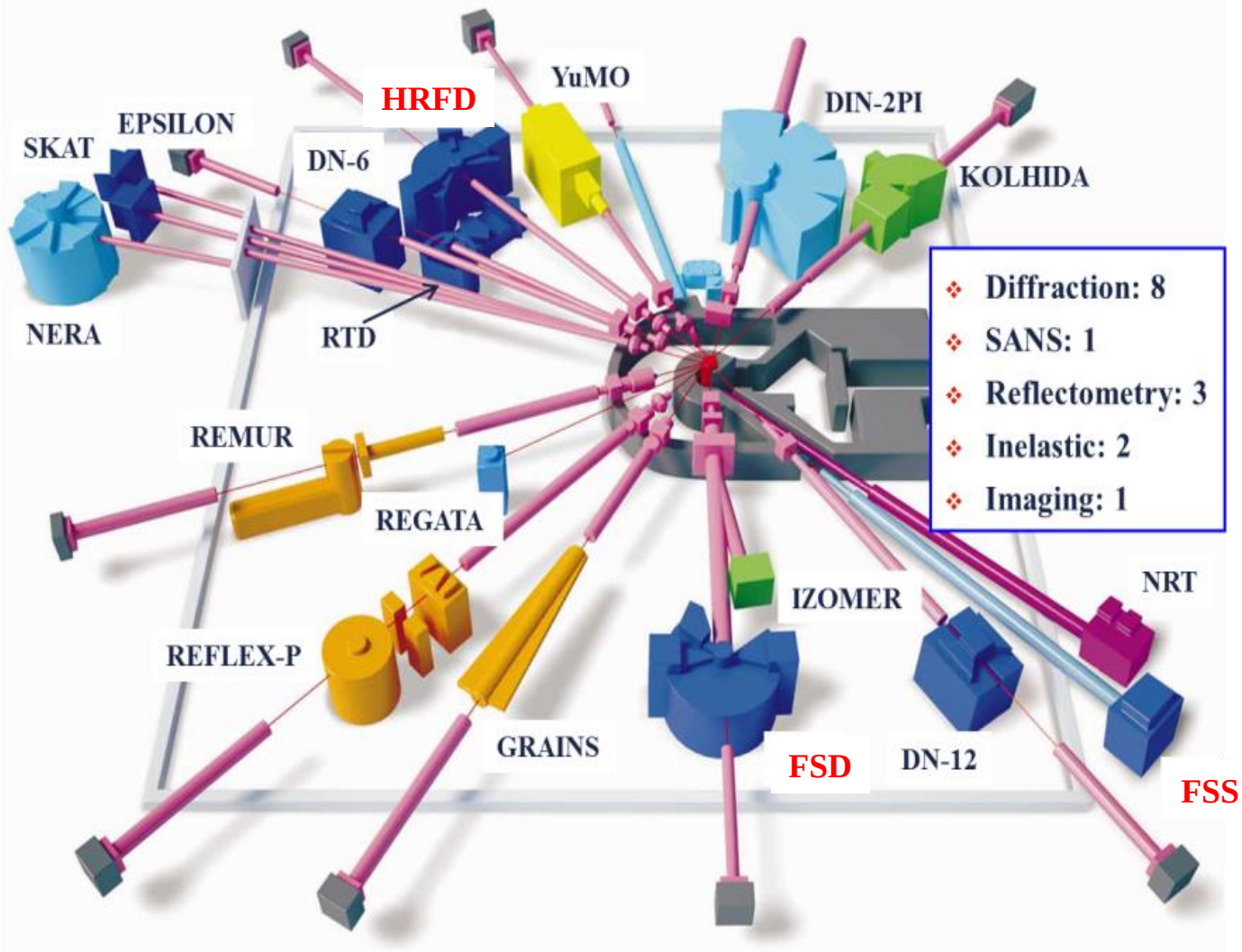

1. HRFD – High Resolution Fourier Diffractometer
   - atomic and magnetic structures
   - thermodiffractometry in real-time mode

2. FSD – Fourier Stress Diffractometer
   - residual stress studies

3. FSS – Fourier Stress Spectrometer
   - residual stress studies

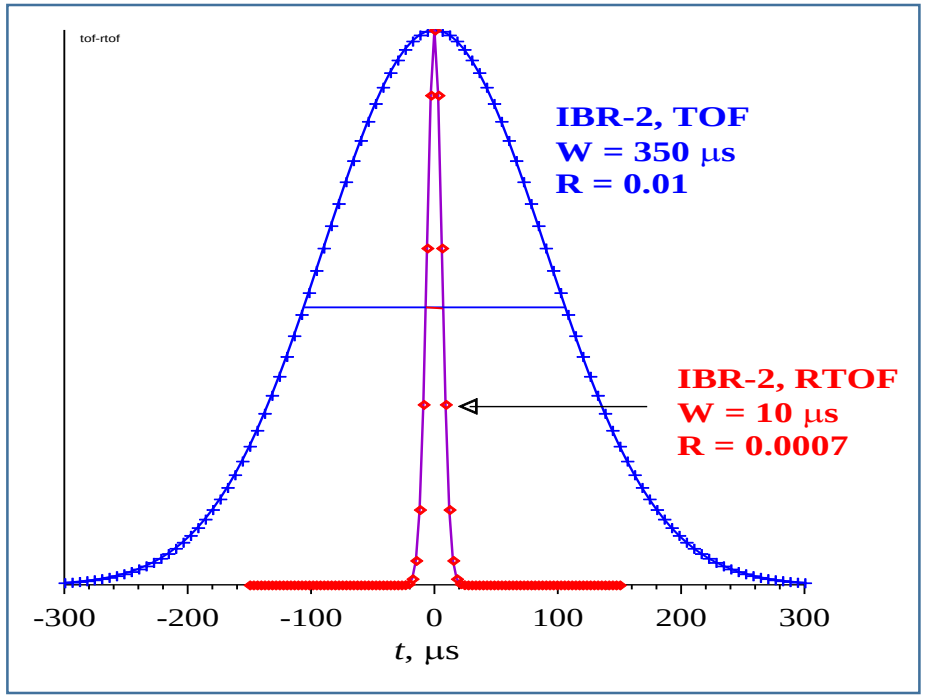

HRFD – High Resolution Fourier Diffractometer
(*Dubna – Gatchina – Espoo collaboration*, 1994)

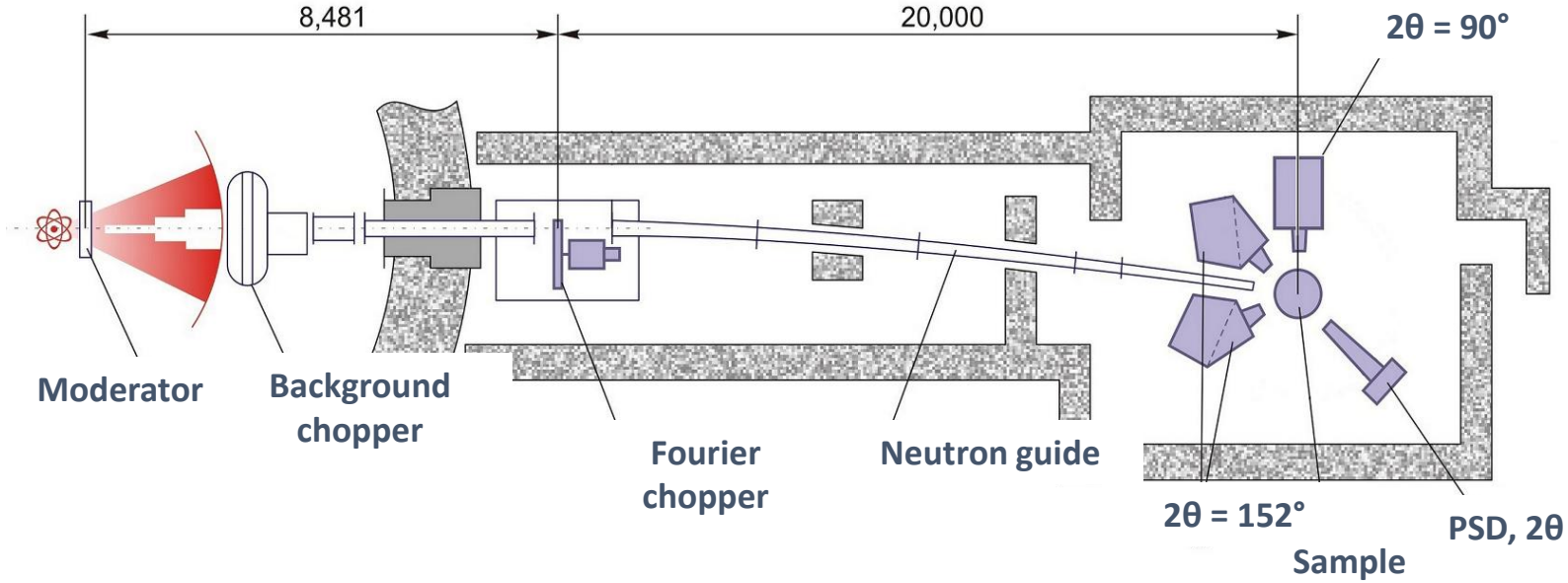

neutron flux	10^7 n/cm^2/s
sample volume	~ 2 cm^3

<u>High-resolution mode</u>:

$\Delta t_0 \approx 10$ μs, $\Delta d/d \approx 0.0015$ for $d = 2$ Å

$\Phi_0 \approx 4 \cdot 10^6$ n/cm^2/s, $t_s \sim 1$ h

<u>High-intensity mode</u>:

$\Delta t_0 \approx 350$ μs, $\Delta d/d \approx 0.015$ for $d = 2$ Å

$\Phi_0 \approx 4 \cdot 10^7$ n/cm^2/s, $t_s \sim 1$ min

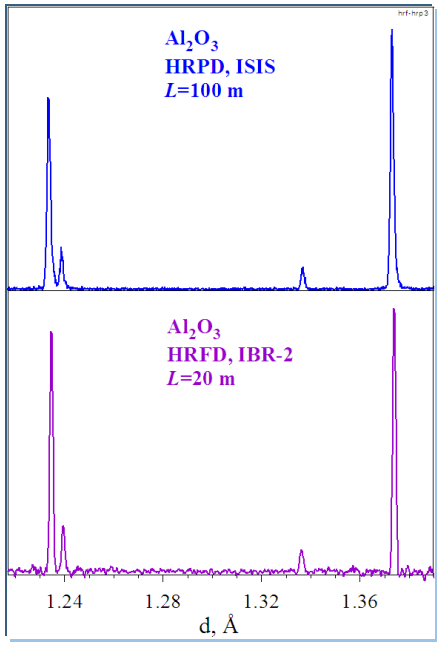

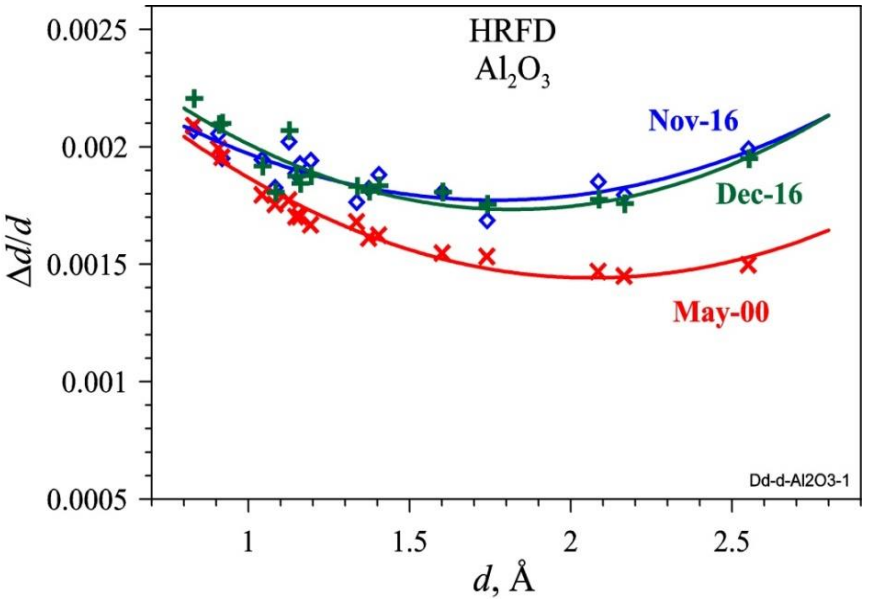

Fast Fourier chopper at HRFD

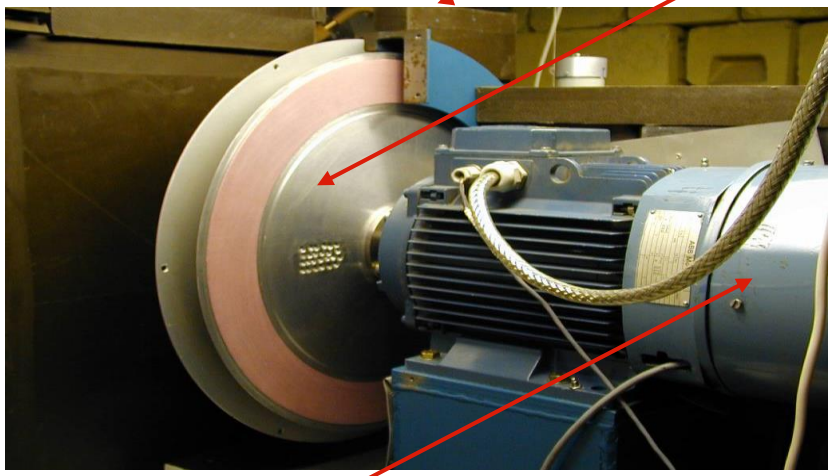

7.5 kW motor

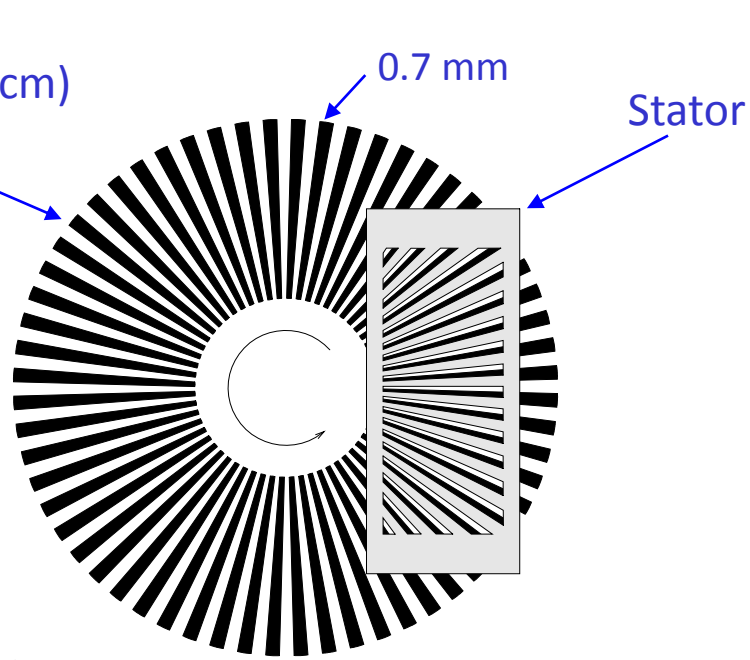

Triangular chopper transmission function:

$T(t) \approx 1 + \sin \omega t$

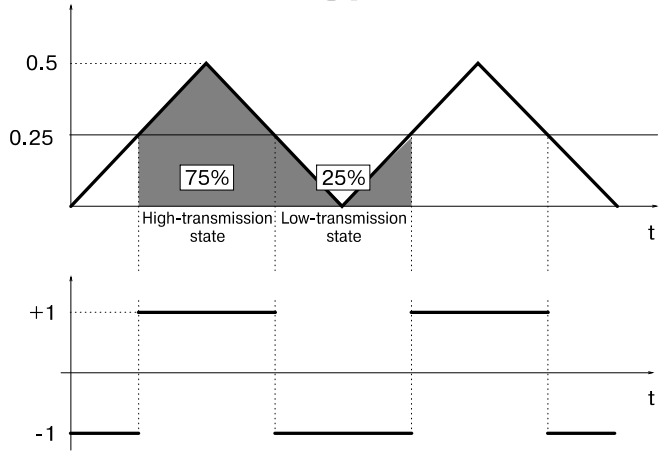

Binary pick-up signals for RTOF analyzer

Dubna chopper:

- Al-alloy
- ∅ = 50 cm
- N = 1024
- $\langle d \rangle$ = 0.7 mm
- V_{max} = 6000 rpm
- Ω = 100 kHz
- Δt_0 = down to 10 μs
- S_{beam} = 3x20 cm^2
- Transmission = 25%

High Resolution Fourier Diffractometer (HRFD)

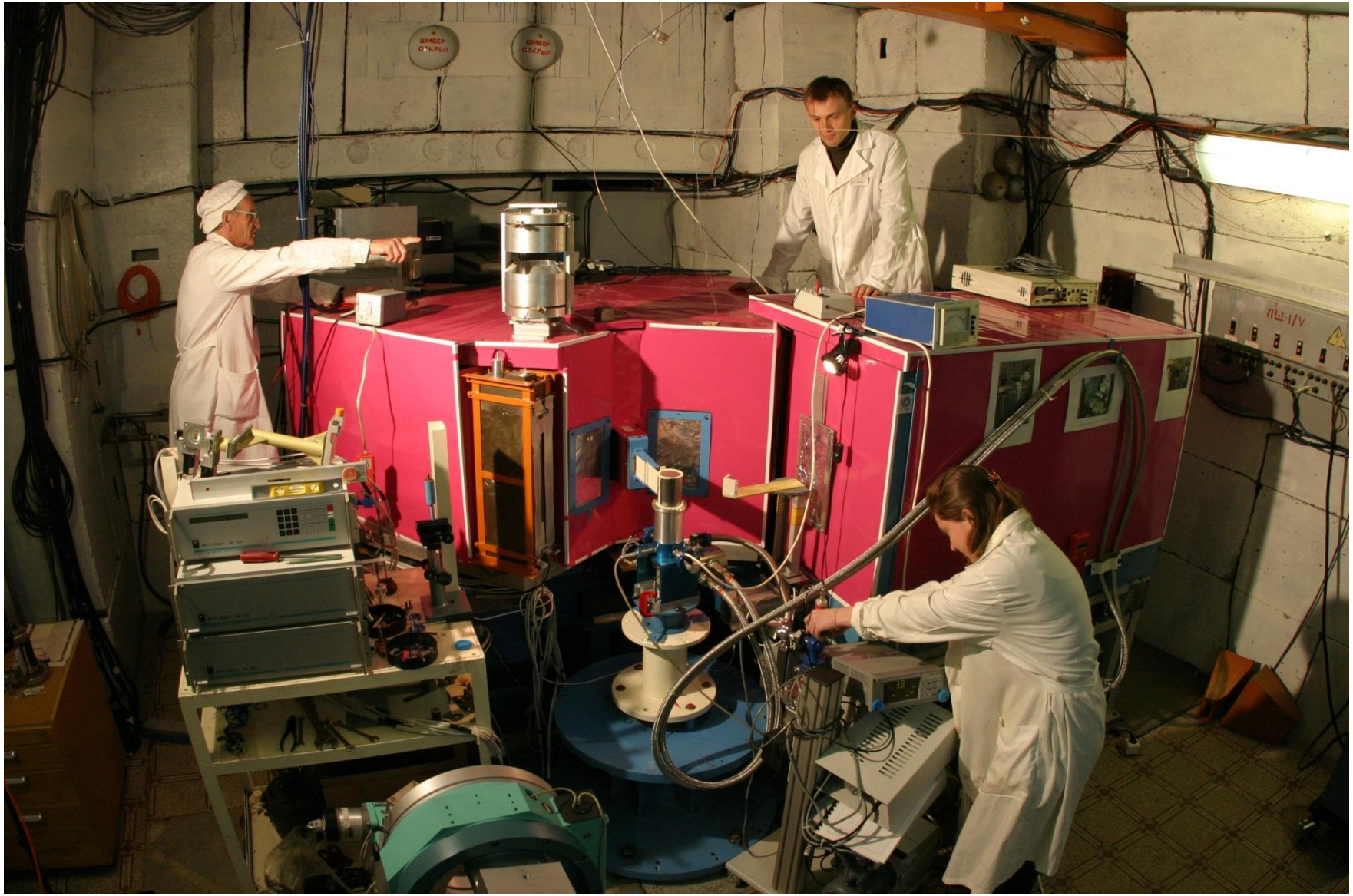

High resolution Fourier diffractometer

To precise study crystal structure and microstructure of crystalline powders

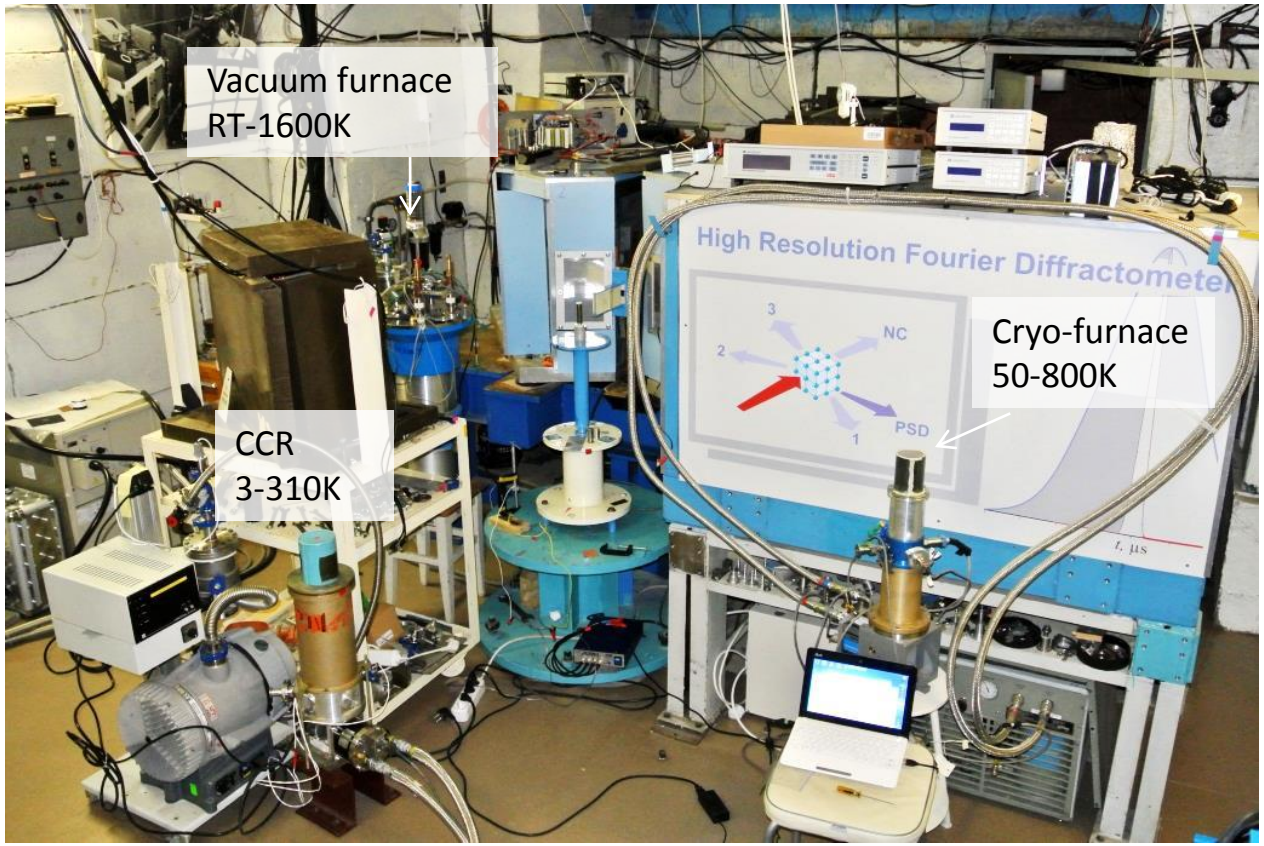

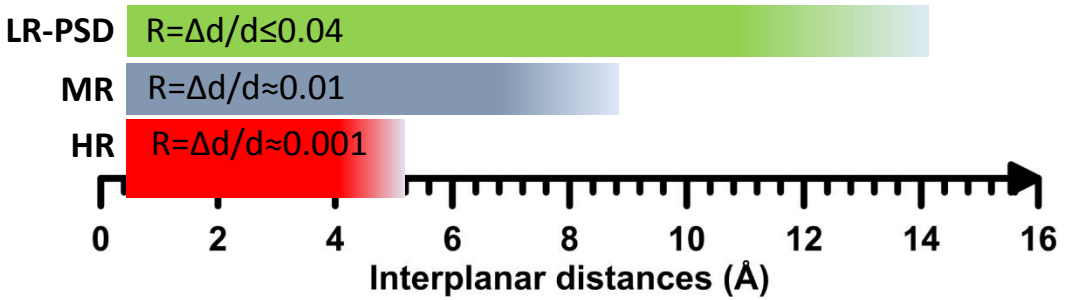

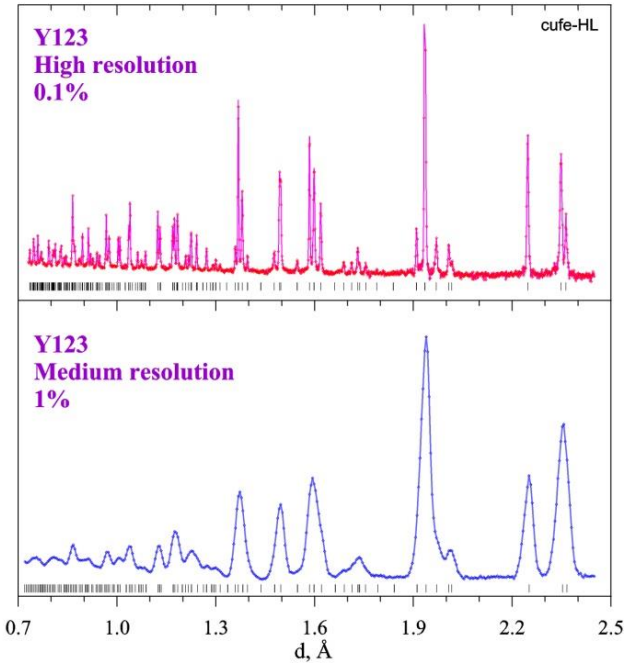

modernization of the HRFD detector system: 2022- 2024

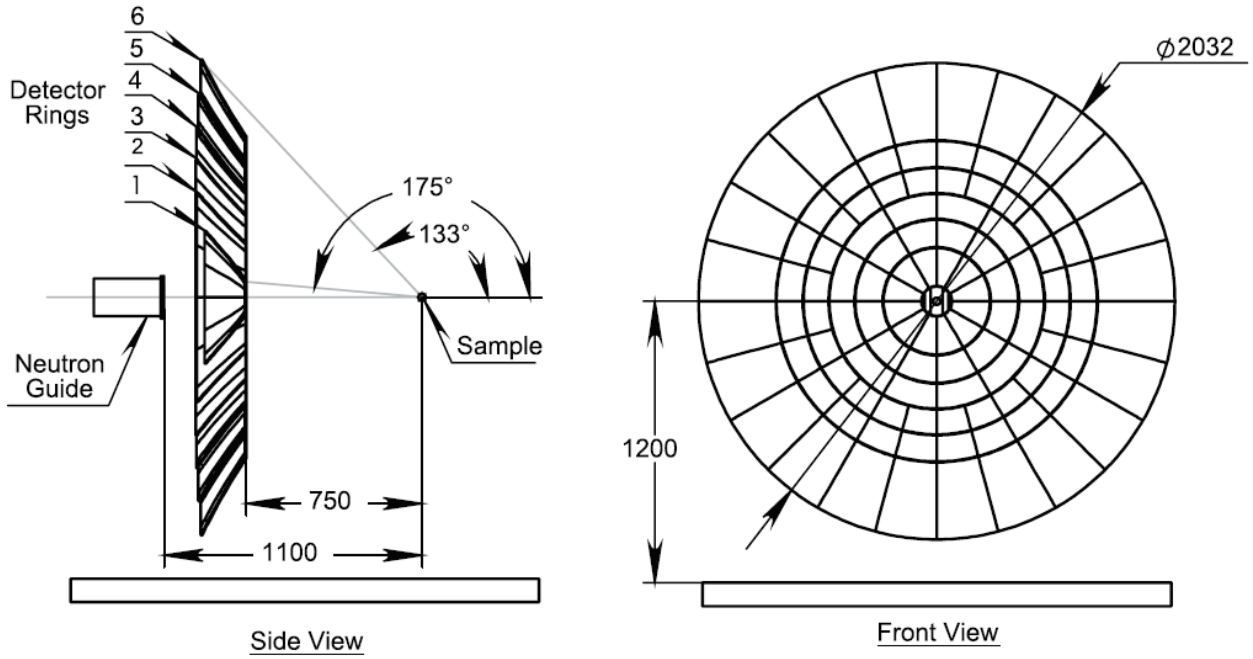

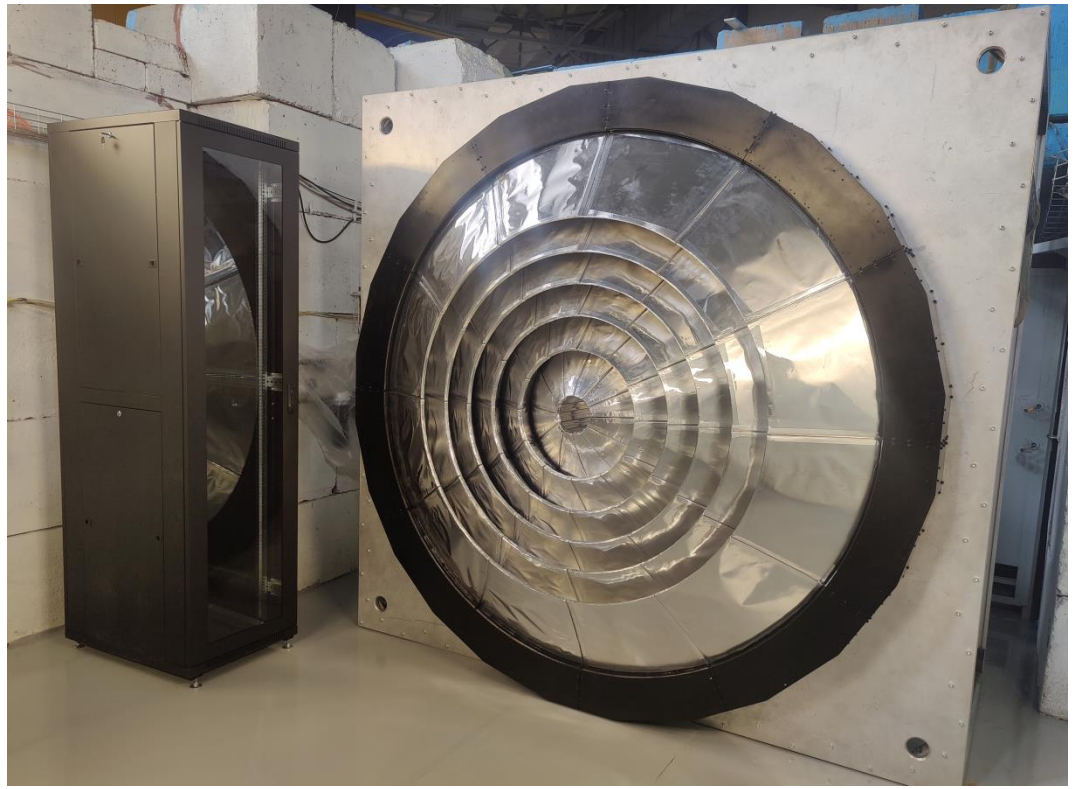

Basic Parameters

type of detector	scintillation ZnS(Ag) with time-focusing geometry
total area of sensitive elements	~13m^2
total solid angle	~2.0 sr (12.5 times greater than the existing one)
thickness of the screens	0.42 mm

Structural and magnetic (spin-flip) phase transitions in Fe_3Ge alloy

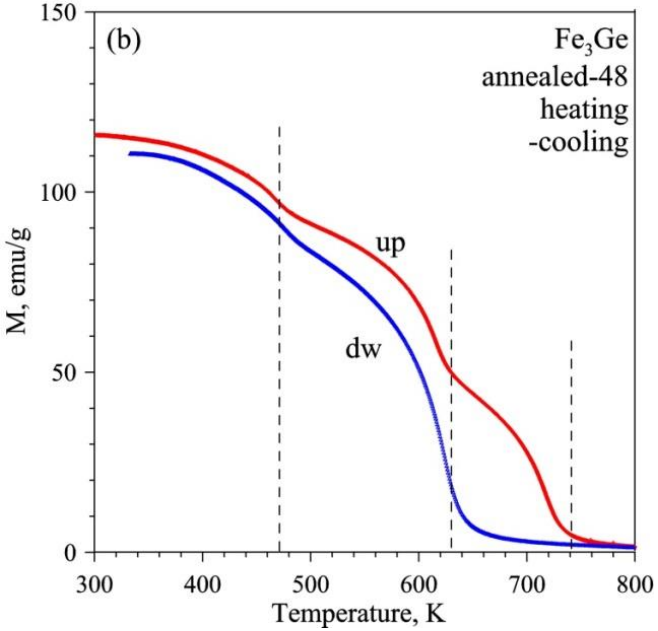

Temperature dependencies of the specific magnetization at heating and cooling.

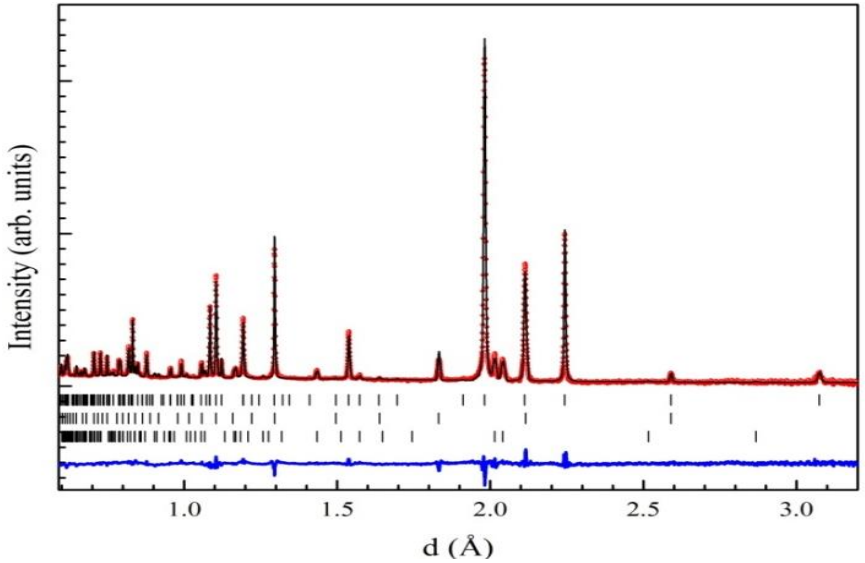

Neutron diffraction pattern (high resolution) collected at RT and processed by the Rietveld method. The vertical bars are calculated peak positions of the $D0_{19}$, $L1_2$, and $B8_2$ phases.

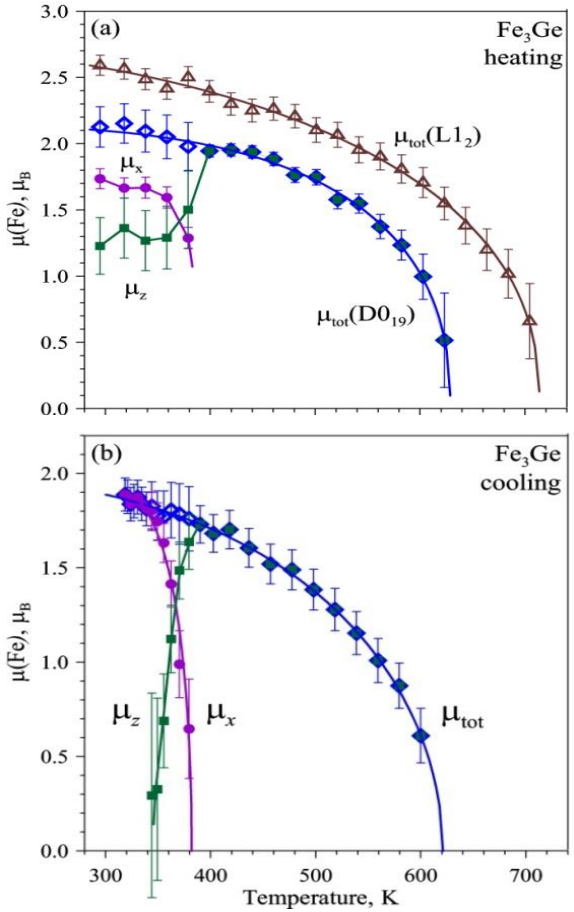

Magnetic moments of the both phases at heating and the $D0_{19}$ phase at cooling. The components in basal plane (μ_x) and along hexagonal axis (μ_z) are shown.

The 2D map of the evolution of the neutron diffraction patterns of the annealed-48 Fe3Ge sample measured *in situ mode upon:* continuous heating up to 1000 K (2 K/min), exposure at this temperature for 1 h, cooling down to 873 K, exposure at this emperature for 4 h, and cooling down to RT (2 K/min).

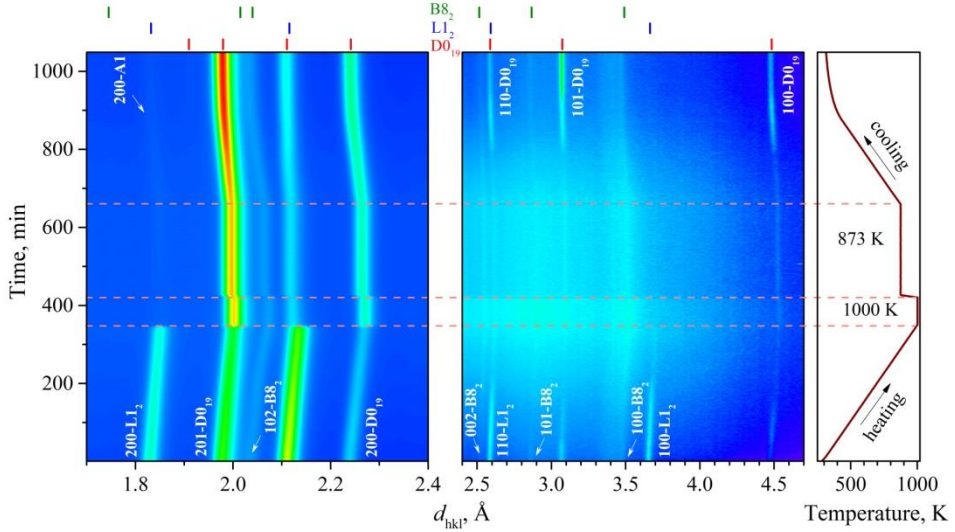

A.M. Balagurov et al. **Physical Review Materials**, 2023

Study of materials for Li-ion power sources at HRFD in real-time mode

$LiFePO_4:V_\delta - Li_xC_6$
based batteries
Size = 8.2 x 128 x 155 mm

V-added ($\delta \approx 1\%$) C ≈ 10 Ah

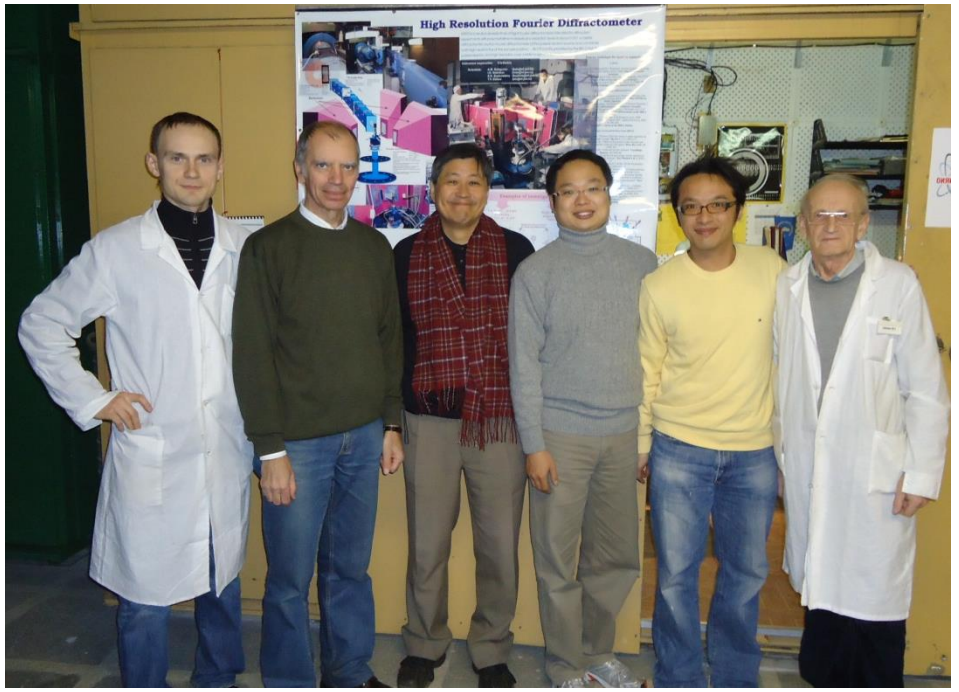

Taiwanese team at HRFD

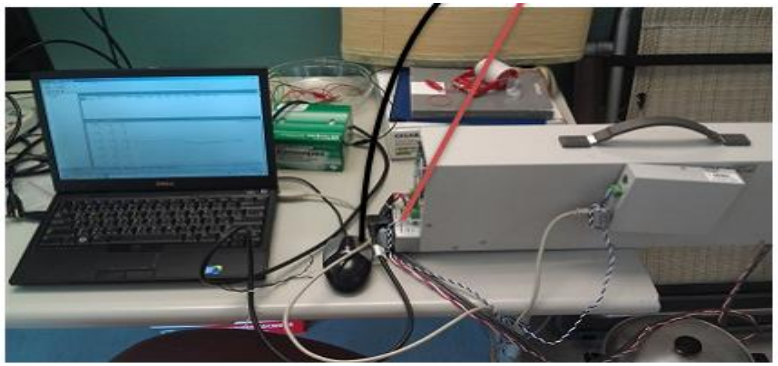

Charge/discharge system
and control PC

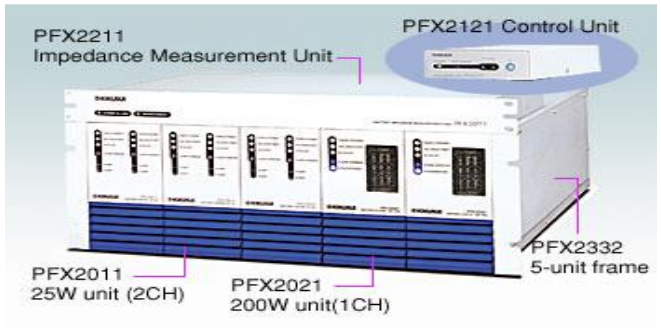

KIKUSUI PFX2011
potentiostat

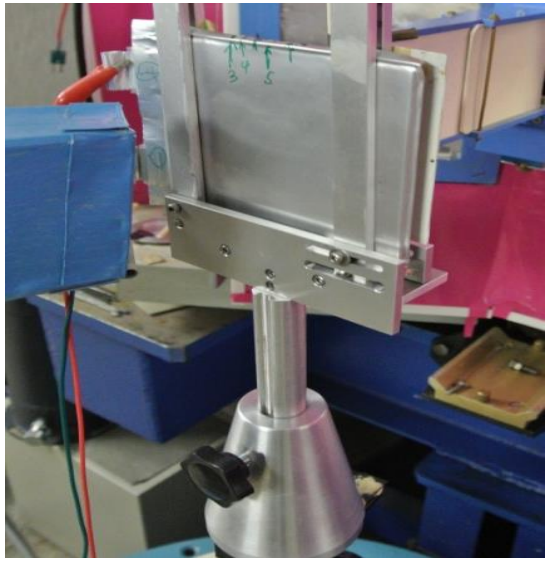

In situ ND of $LiFePO_4$-based battery

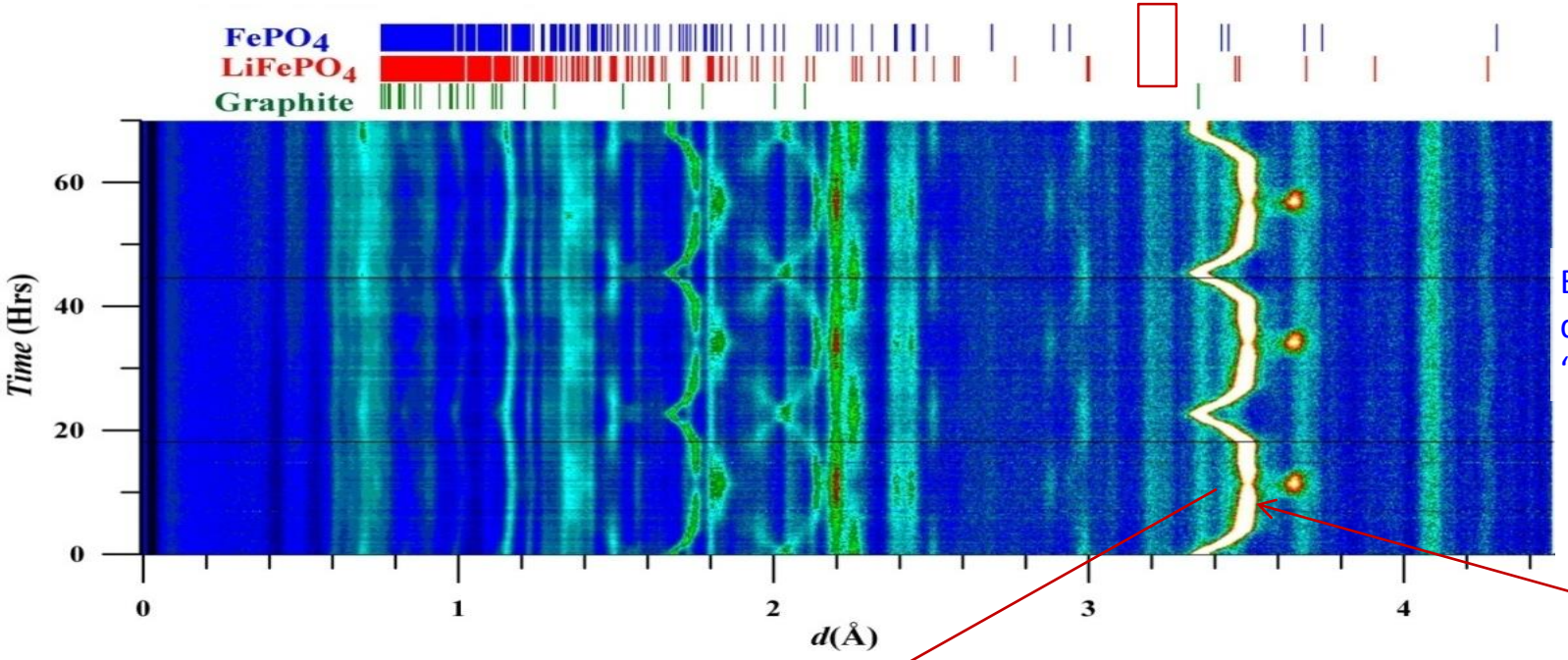

Evolution of the neutron diffraction patterns measured during three charge/discharge (~70 hours) cycles.
"Anode window" is marked.

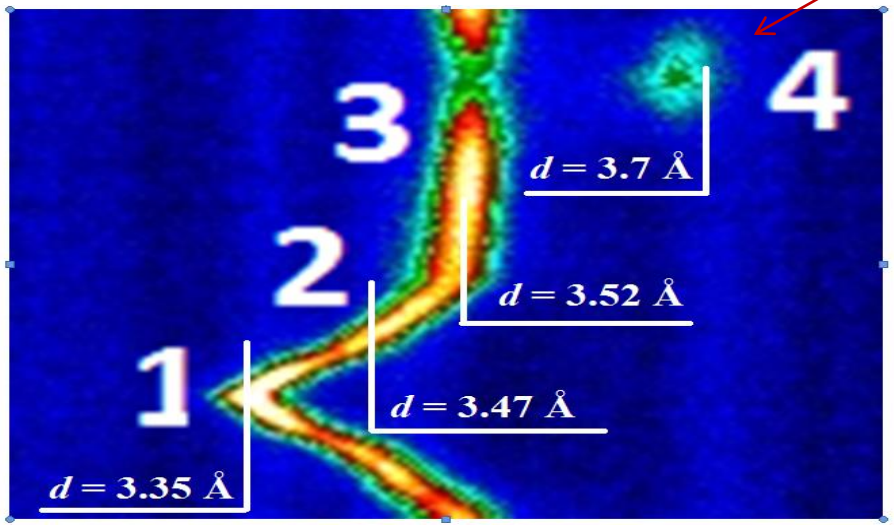

Enlarged chart of the initial (discharged) state with pure graphite line (d = 3.35 Å) and stepwise appearance of LiC_{24} (d = 3.47 Å) and LiC_{12} (d = 3.47 Å).

3D view of the "anode-window" region for all three cycles of charge/discharge processes

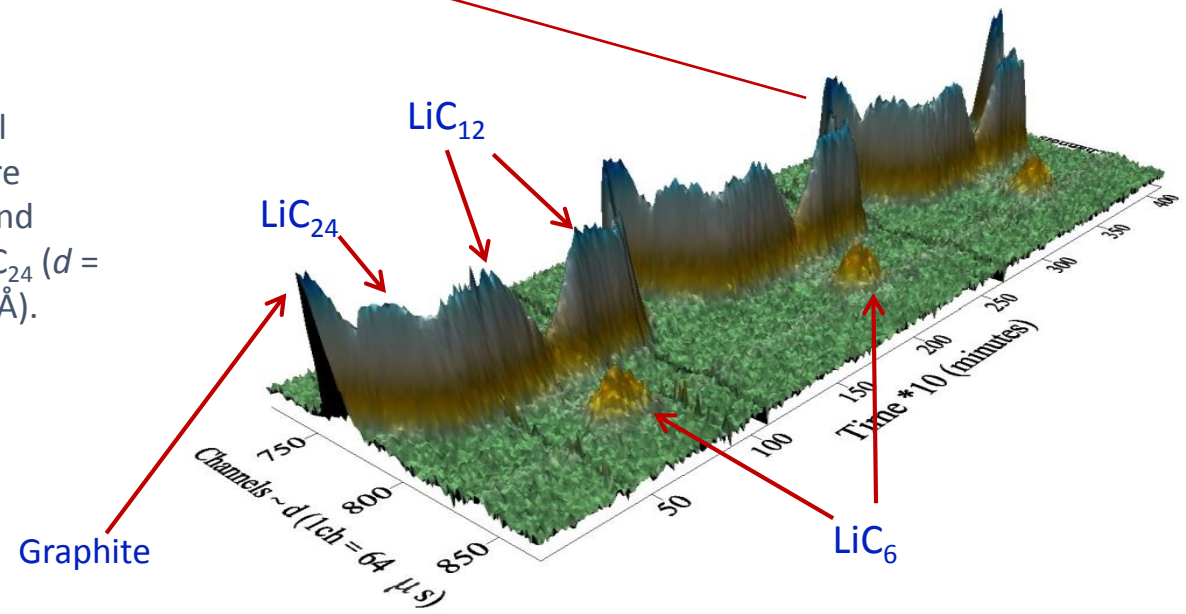

Operando study of phase separation in $LiNi_{0.8}Co_{0.15}Al_{0.05}O_2$

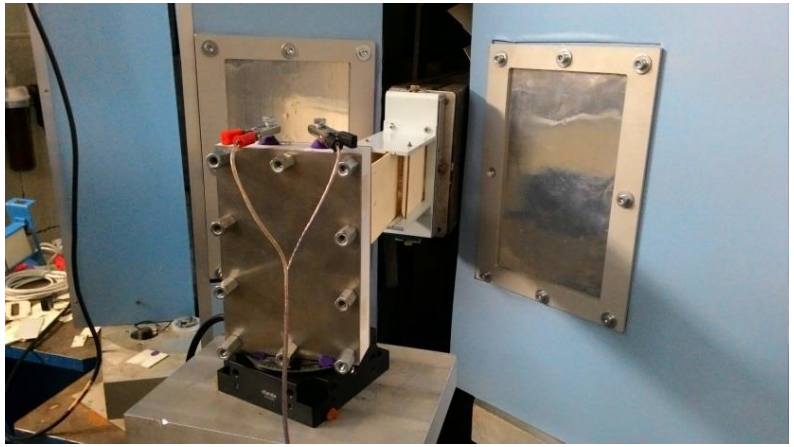

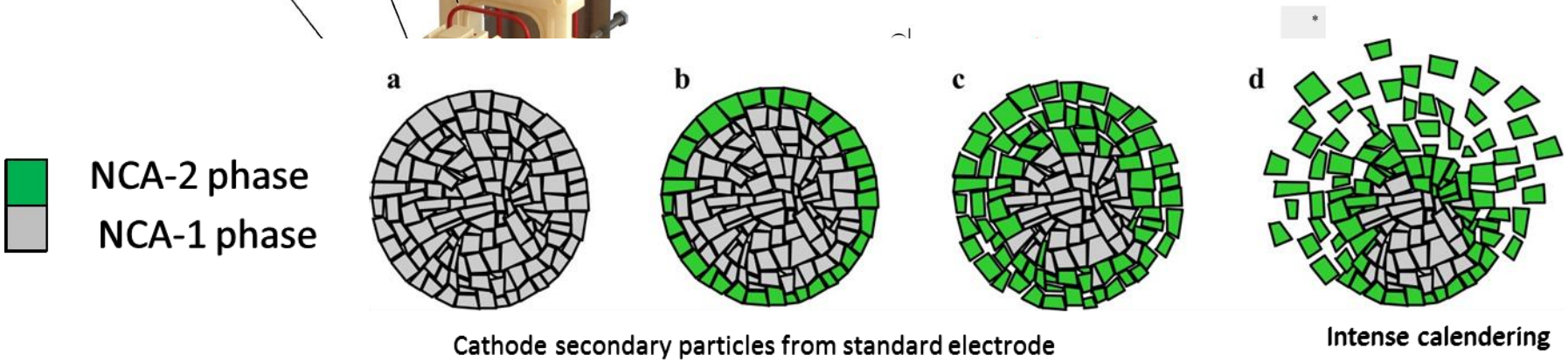

1) Easy to assembly
2) Si window for neutrons
3) "Beam stop"
4) Li-metal as counter electrode

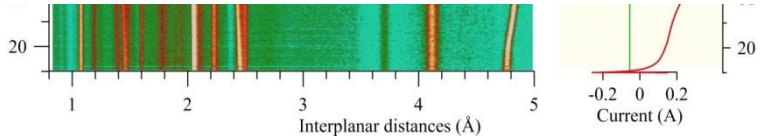

Bobrikov et al. Electrochimica Acta 2018

Electrochemical laboratory development

Some equipment:

1. Metrohm Fischer titrator 917
2. Despergator up to 25000 rpm and other mixers
3. Potentiostat BIOLOGIC SP-300
4. High temperature inert gas furnace up to 1200˚ C
5. Storage of d-electrolytes for neutron scattering experiments (DMC, PC, EC)
6. 3-axes stage for non-standard samples and electrochemical cells at X-ray diffractometer,
7. Glove box with atmosphere controlling systems etc.

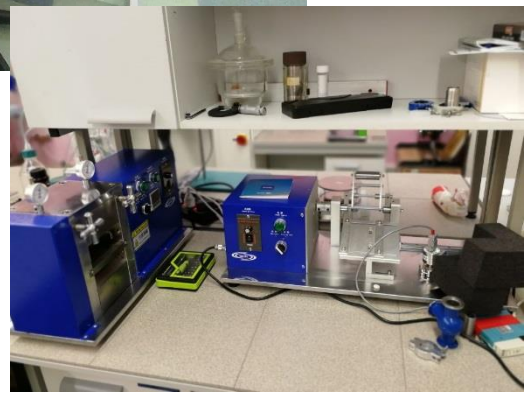

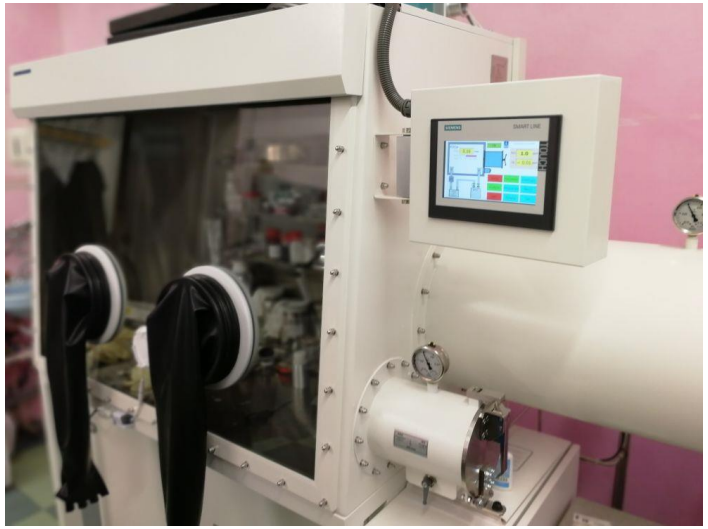

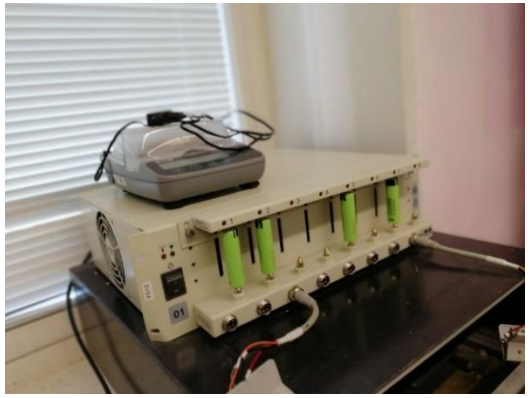

Bobrikov et al, 2019

Intermetallic Fe-based compounds with giant magnetostriction

Collaboration

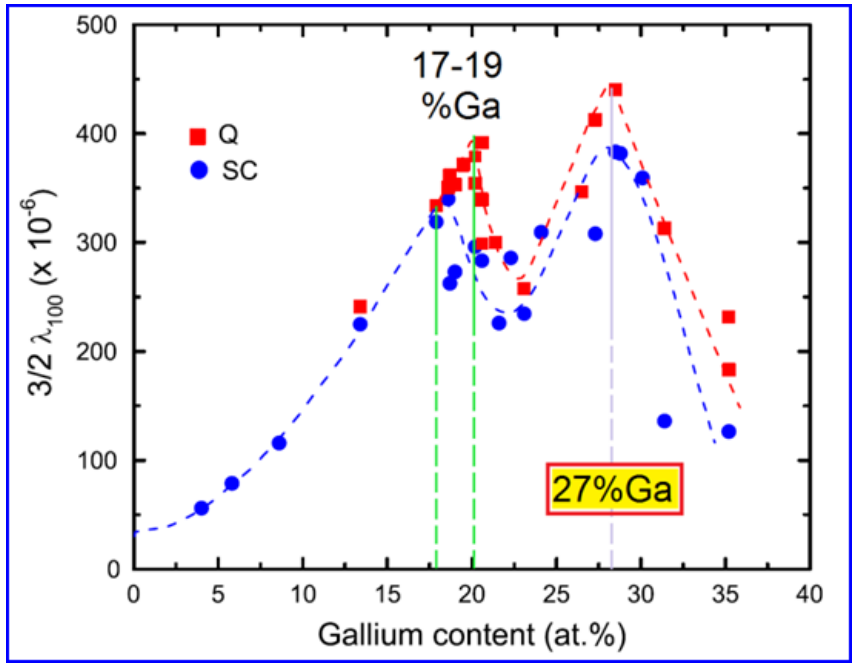

Equilibrium

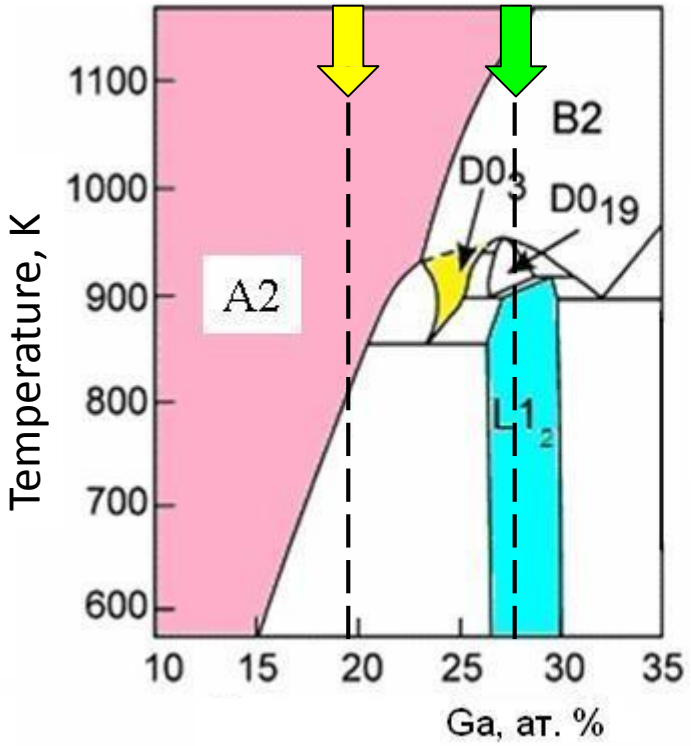

Non equilibrium

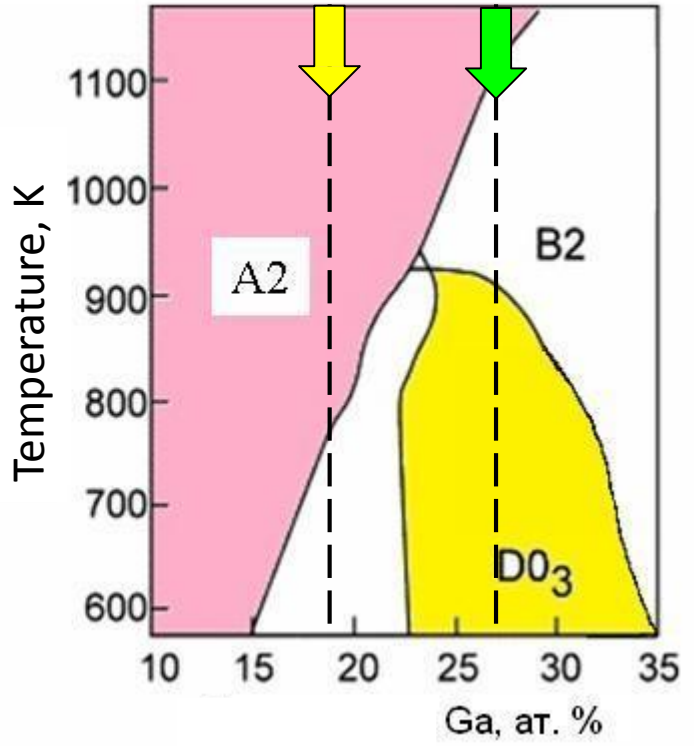

Phase transitions in Fe-27Ga-RE, RE = Dy, Er, Tb, Yb

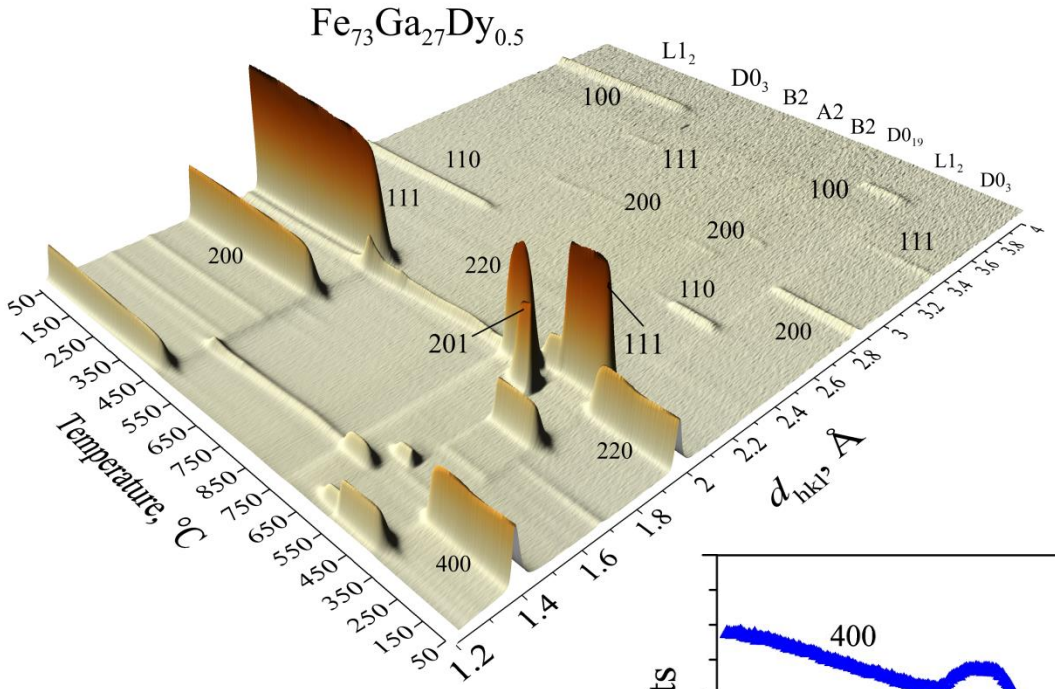

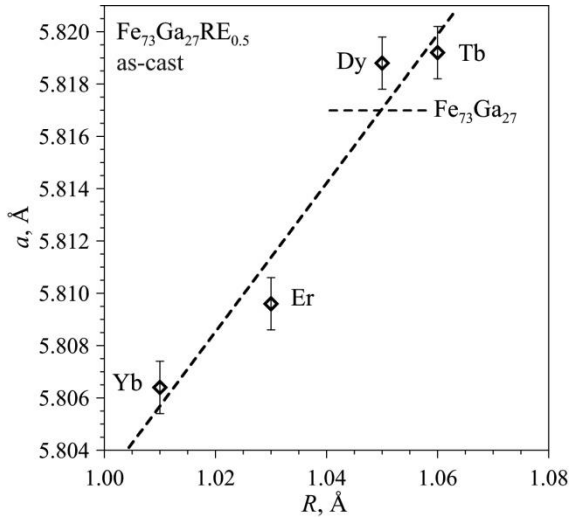

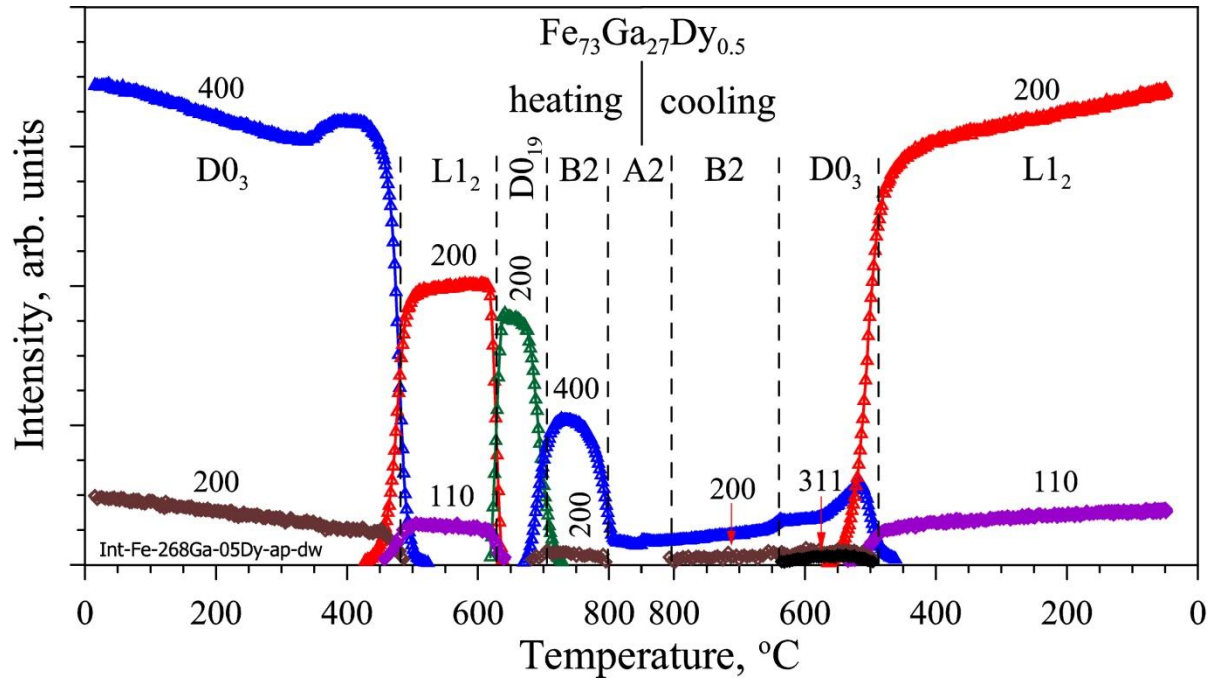

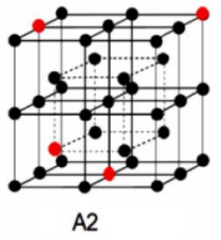

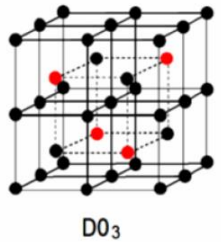

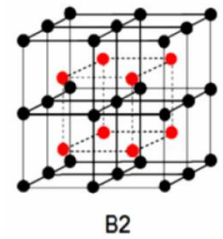

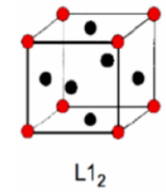

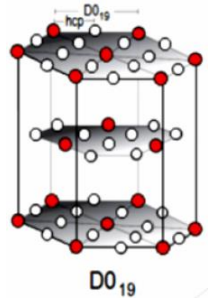

The isothermal phase transitions in Fe3Ga-type compounds

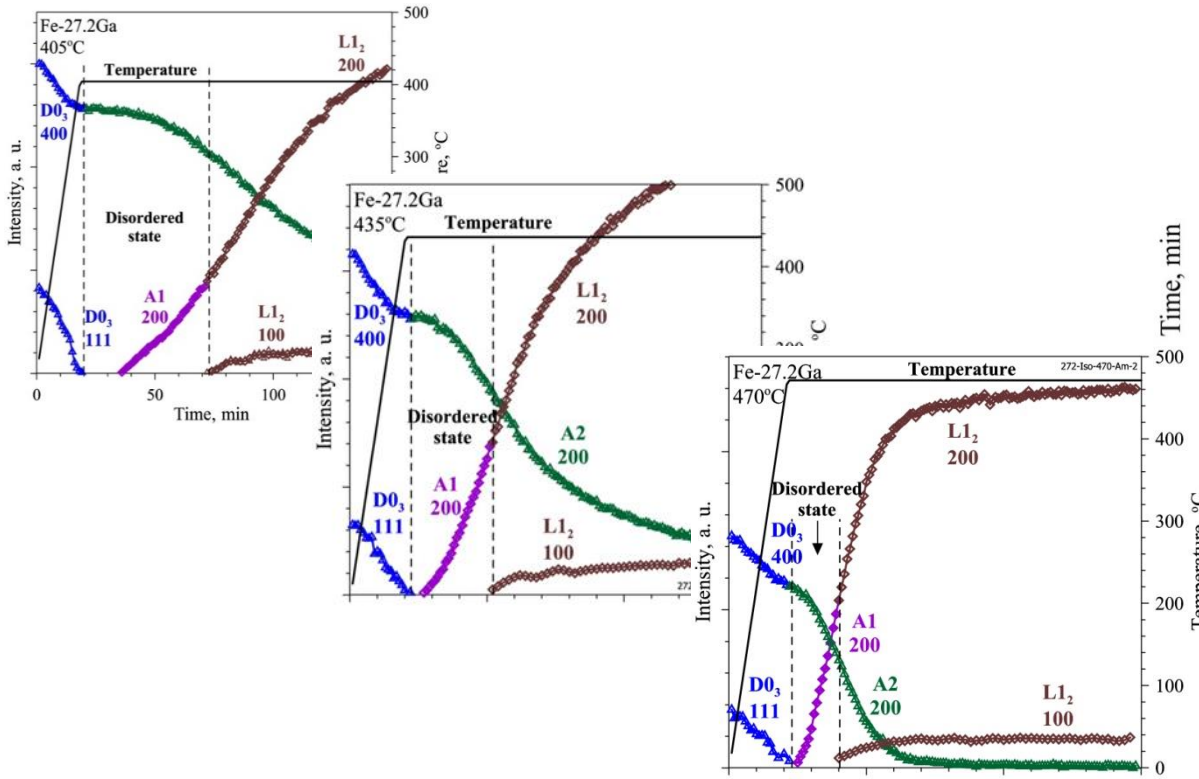

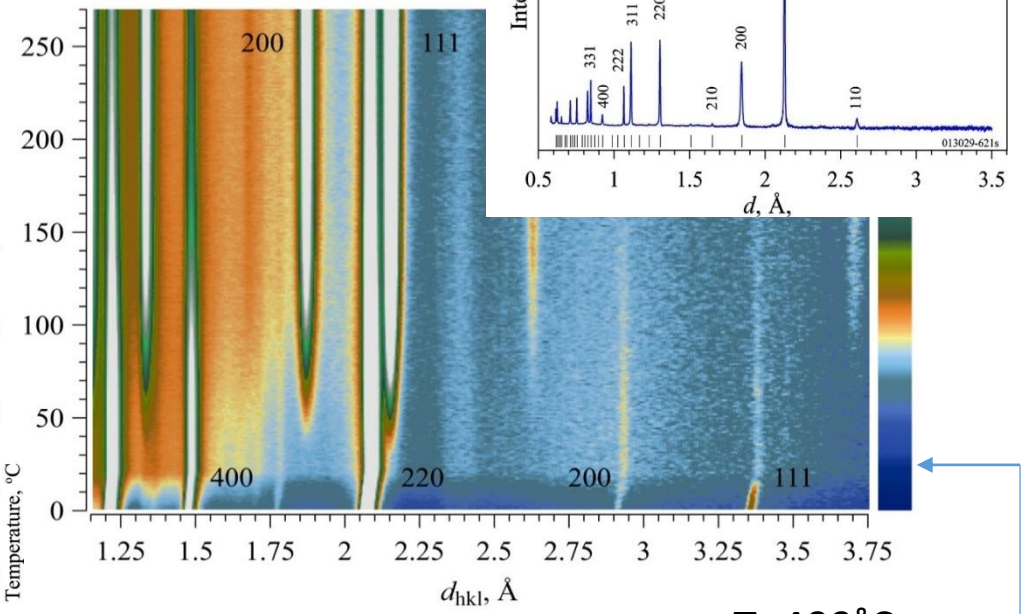

T=409˚C

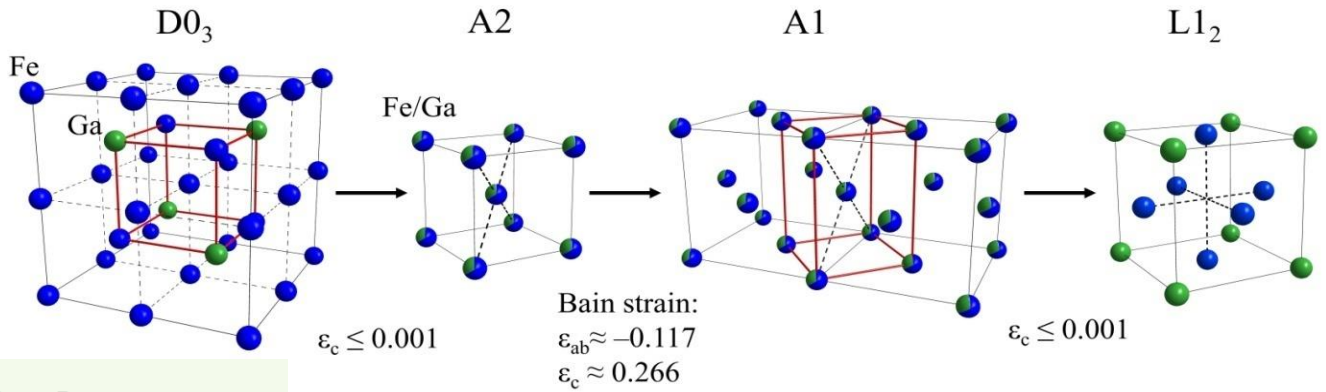

Acta Crystallographica Section B
STRUCTURAL SCIENCE, CRYSTAL ENGINEERING AND MATERIALS

Cluster structure of phase separated state of Fe-27Al and Fe-27Ga

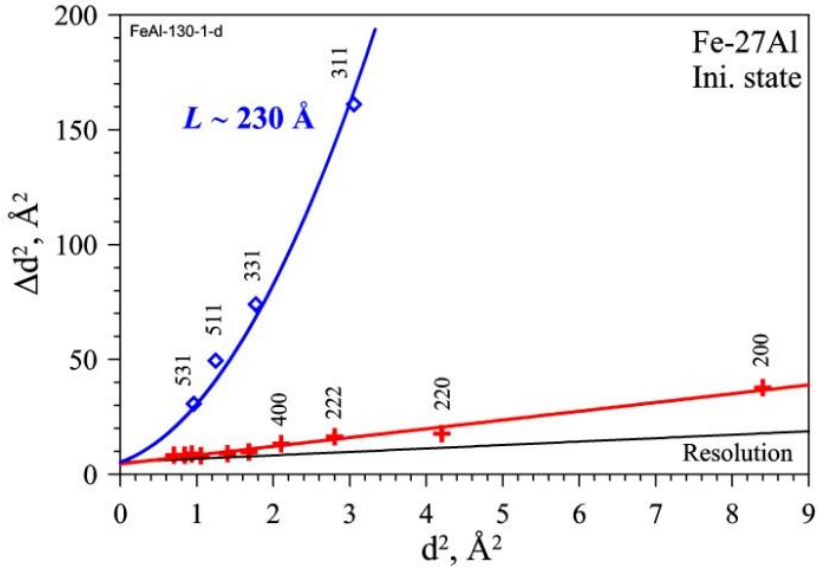

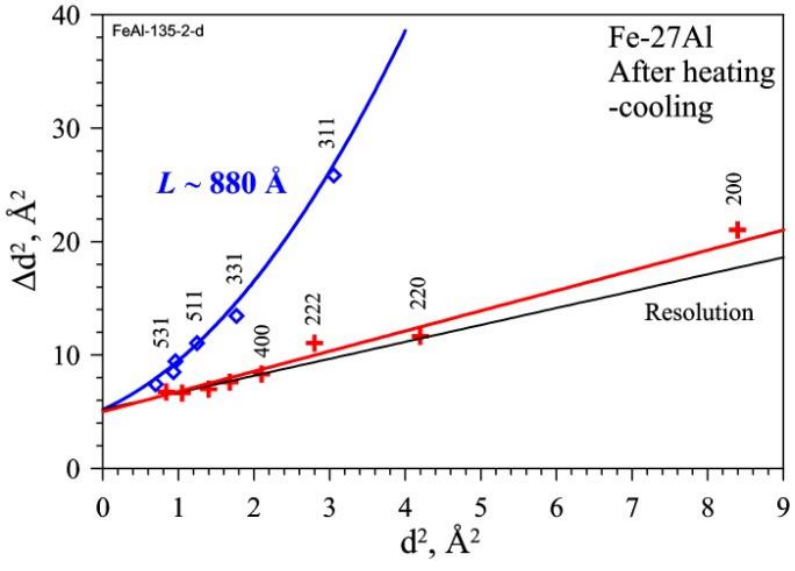

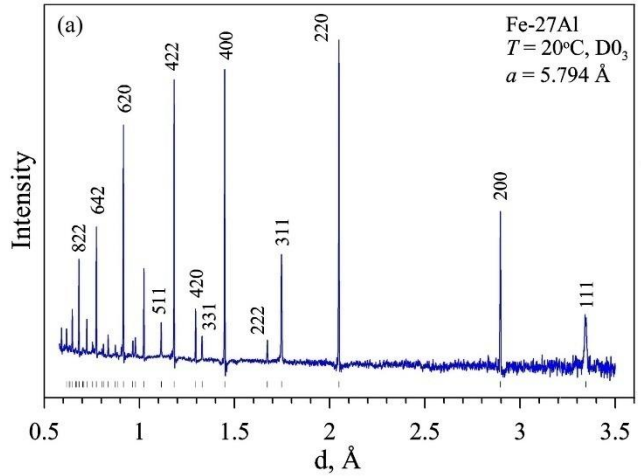

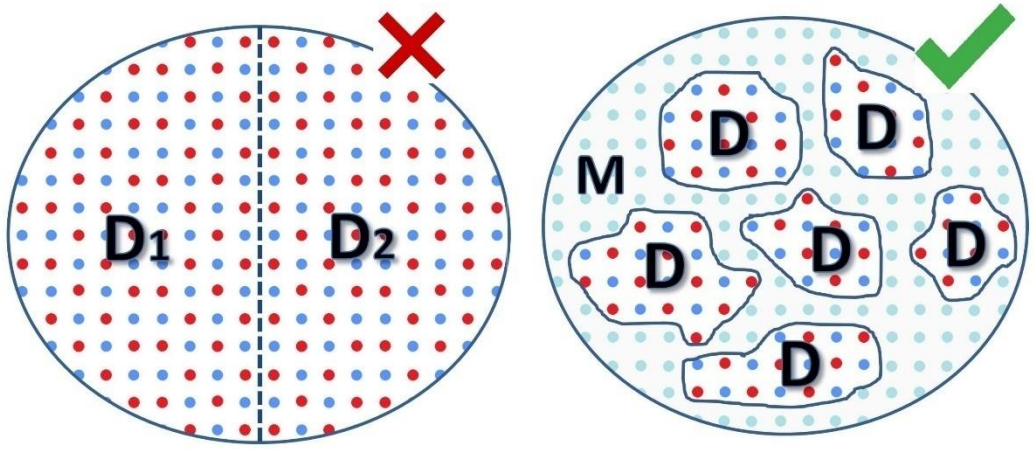

Balagurov, A.M., Bobrikov, I.A., Sumnikov, S.V., Golovin, I.S., (2018) Acta Materialia 153 P.45.

Thanks for your attention!

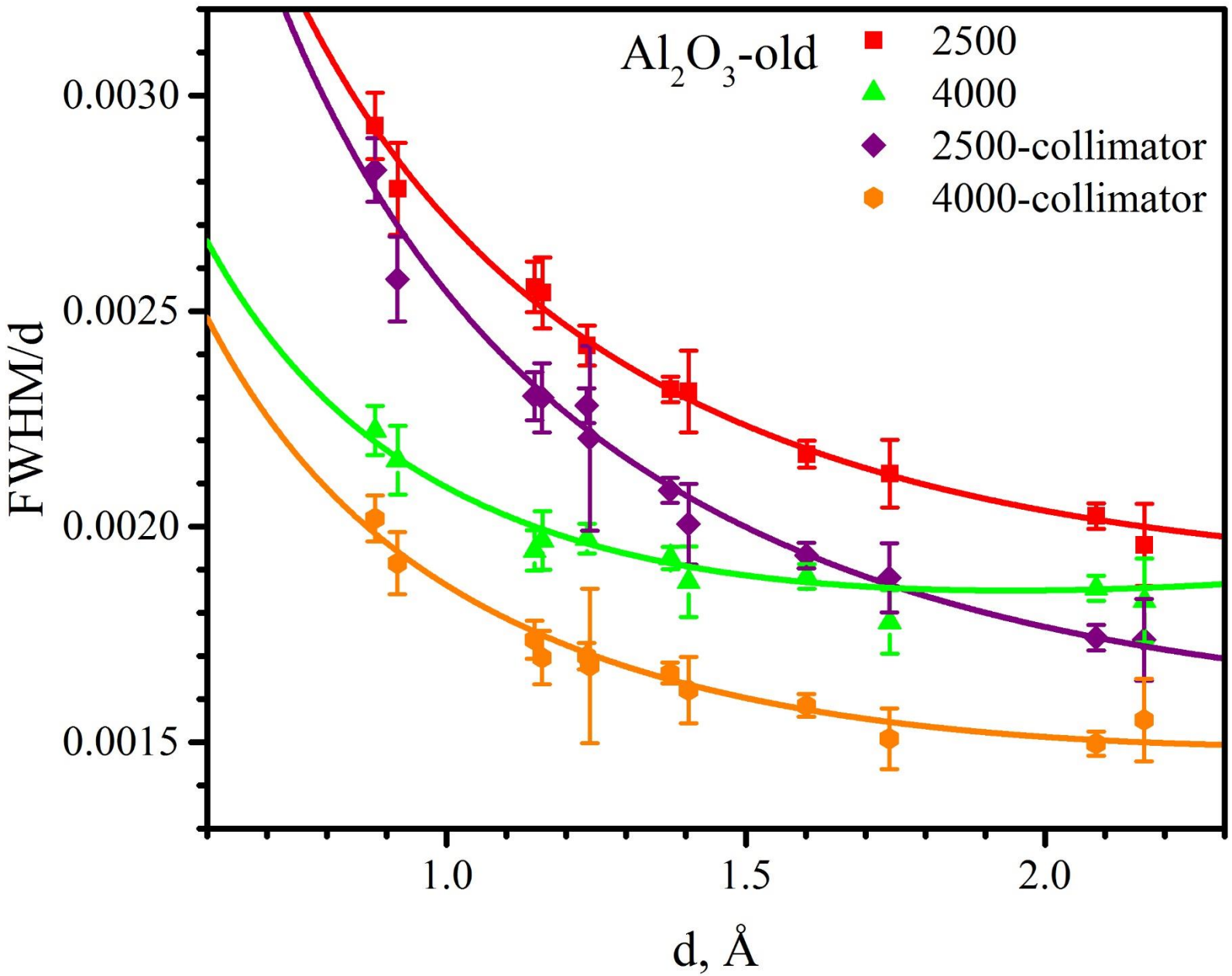
Al2O3-old
2500
4000
2500-collimator
4000-collimator
FWHM/d
0.0030
0.0025
0.0020
0.0015
1.0
1.5
2.0
d, Å